

Colorimetric Sensor Based on Self-Assembled Polydiacetylene/Graphene-Stacked Composite Film for Vapor-Phase Volatile Organic Compounds

Xiaona Wang, Xiuling Sun, Ping An Hu,* Jia Zhang, Lifeng Wang, Wei Feng, Shengbin Lei, Bin Yang, and Wenwu Cao

A portable litmus-type chemosensor is developed for the effective detection of environmentally hazardous volatile organic compounds (VOCs) using polydiacetylene (PDA) and graphene stacked within a composite film. The graphene is exploited as a transparent and efficient supporter for the highly ordered PDA monolayer. This colorimetric sensor exhibits a sensitive response to low concentrations of VOCs (~0.01%), including tetrahydrofuran (THF), chloroform (CHCl₃), methanol (CH₃OH), and dimethylformamide (DMF). The color change that is caused by relatively high concentrations of VOCs can be perceived by the naked eye, and it is noteworthy that a logarithmic relationship is observed between the chromatic response and the VOC concentration in the range of ~0.01%–10%. The structural conformation changes of the PDA molecules, caused by interactions with VOCs, are directly observed by scanning tunneling microscopy (STM), which reveals the intrinsic mechanism of the chromatic variety at the molecular level.

1. Introduction

Polydiacetylenes (PDAs) are π -conjugated polymers that can be prepared by the UV irradiation of self-assembled diacetylene (DA) supramolecules. They have attracted considerable attention in recent years due to their application potential in chemical sensors.^[1–3] PDAs exhibit intense chromatic variation from blue to red in response to external stimuli, such as temperature, solvent, mechanical stress, and ligand–receptor interactions.^[4–7] These colorimetric changes can be quantified by UV–vis

absorption and fluorescence spectroscopy, and they can even be perceived by the naked eye, which make PDA a promising material for the development of colorimetric sensors with the desired characteristics of simplicity and portability.^[8–10] Volatile organic compounds (VOCs) are well-known environmental pollutants, which have been causing human chronic immune diseases and the extinction of many biological species. Current analytic techniques of VOCs in water or atmosphere include liquid and gas chromatography, metal oxide sensors, metal organic framework sensors, and surface acoustic wave devices.^[11–13] These methods suffer the disadvantages of high cost and tedious or complex preparation procedures. In order to obtain portable and more efficient

analytic sensors for VOCs, recent attention has been focused on PDA-based colorimetric sensors.

PDA sensors are made in the form of vesicles, liposomes, Langmuir–Blodgett (LB) films, casting films, or nanocomposites. At first, most PDA-based sensors for VOCs or other analytes were demonstrated using PDA aqueous suspensions or thin films (LB or Langmuir–Schaefer (LS)) on solid substrates. Subsequently, to overcome the poor stability associated with solution- or film-based sensors, PDA materials were embedded in host polymer matrices in various forms, such as polyethylene oxide electrospun fibers, casting films of carbohydrates,^[14] poly(vinylpyrrolidone) (PVP),^[15] and poly(vinyl alcohol) (PVA).^[16] Zhang and co-workers have developed a PDA-embedded polydimethylsiloxane (PDMS) colorimetric microarray sensor for the detection and identification of VOCs.^[17] Recently, PDA supramolecules were immobilized onto the surfaces of membrane filters, silica microbeads, and glass fibers, aiming to make the handling of colorimetric polymer sensors easier.^[18–23] Wacharasindhu and co-workers have fabricated a system where PDA is deposited onto a filter-paper surface using the drop-casting technique; color change patterns were generated upon exposure to VOC vapors, which can be measured by the RGB (red–green–blue) values and statistically analyzed.^[24] However, there are still some existing problems in such sensors, such as low sensitivity, the inability for precise quantitative analysis, and an unclear sensing mechanism. In other words, current PDA sensors still need further

Dr. X. N. Wang, Dr. X. L. Sun, Prof. P. A. Hu,
Dr. J. Zhang, Dr. L. F. Wang, Dr. W. Feng, Prof. S. B. Lei
Key Lab of Microsystem and Microstructure of
the Ministry of Education
Harbin Institute of Technology
Harbin, 150080, China
E-mail: hupa@hit.edu.cn

Dr. X. N. Wang, Prof. P. A. Hu, Dr. L. F. Wang, Dr. W. Feng
Department of Material Physics and Chemistry
Harbin Institute of Technology
Harbin, 150080, China

Prof. B. Yang, Prof. W. W. Cao
Condensed Matter Science and Technology Institute
Harbin Institute of Technology
Harbin, 150080, China



DOI: 10.1002/adfm.201301044

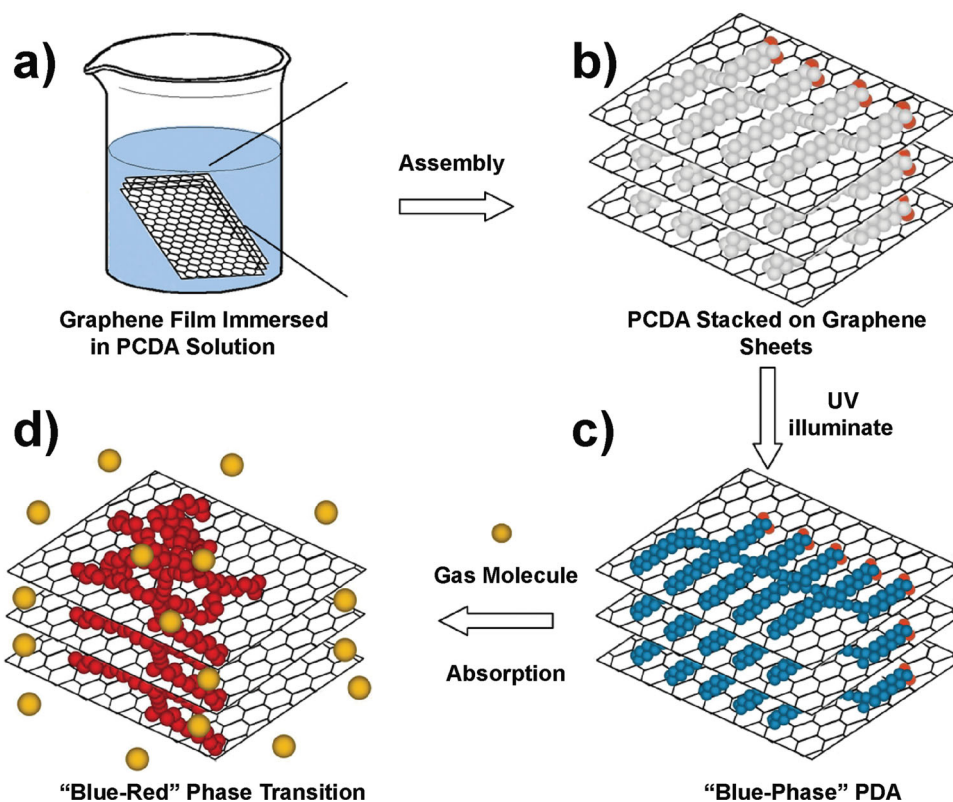


Figure 1. a) Schematic showing the preparation of the composite films and b–d) the molecular arrangement of how the PDA film self-assembles on graphene starting with PCDA: before (b) and after (c) polymerization, and upon exposure to VOC vapors (d).

improvement in their sensitivity and application to quantitative analysis, and a better understanding of the colorimetric sensing mechanism remains a concern.

In this investigation, we demonstrate PDA-based colorimetric sensors using graphene as a transparent and efficient supporter; the sensors have high sensitivity and a short response time in the detection of VOC vapors. Graphene, which is a flat monolayer of carbon atoms packed into a 2D honeycomb lattice, has a large theoretical specific surface area ($2630 \text{ m}^2 \text{ g}^{-1}$), high chemical stability, ultrahigh mechanical stiffness (a Young's modulus of $<1.0 \text{ TPa}$), good optical transmittance ($<97.7\%$), and good electrical conductivity.^[25] Using graphene as the supporter for the PDA-based colorimetric sensor has several advantages. First, ordered monolayer PDA supermolecules can efficiently form on the large surface of a graphene sheet, similar to the previously reported PDA assembly on highly oriented pyrolytic graphite (HOPG).^[26,27] This amplifies the absorbing area of gaseous molecules. Second, graphene is highly transparent in the UV–vis range, so that the signal of the chromatic change from each PDA monolayer that is immobilized on the graphene sheet in the stacked films can be efficiently detected by spectroscopy. Third, graphene exhibits good chemical and mechanical stability. All of these features form a unique combination that enhances the colorimetric signal of PDA, enabling the detection of low concentrations of VOCs. In addition, monitoring color changes with graphene-immobilized PDA membranes can be

more easily accomplished than those PDA systems where they are embedded in a polymer matrix^[17] or in conventional PDA vesicles.^[28] Kim and co-workers have also developed multifunctional polydiacetylene/graphene nanohybrids for biosensor applications using the self-assembly of PDA on reduced graphene oxide.^[29] AOC sensor based on a PDA/graphene composite film however has not been previously reported.

2. Results and Discussion

The typical procedure for the fabrication of colorimetric sensors based on PDA/graphene composite films is schematically illustrated in **Figure 1**. Graphene flakes with a thickness of ~ 1 – 5 layers were prepared by solvent-sonication-based exfoliations of expanded graphite (shown in Figure S1 in the Supporting Information (SI)).^[30] The graphene film on the polyethylene terephthalate (PET) substrate was prepared by casting or by the PDMS-based imprinting approach (Figure 1a). Commercially available DA of 10,12-pentacosadiynoic acid (PCDA) was selected for this study. The self-assembly of PCDA onto each graphene sheet was accomplished by putting the graphene film into the PCDA solution (Figure 1a,b). The assembled PCDA on the graphene sheets are converted into an ordered PDA film under the illumination of UV light ($\lambda = 254 \text{ nm}$; Figure 1c). The polymerized PDA/graphene can be used for sensing VOC vapors (Figure 1d).

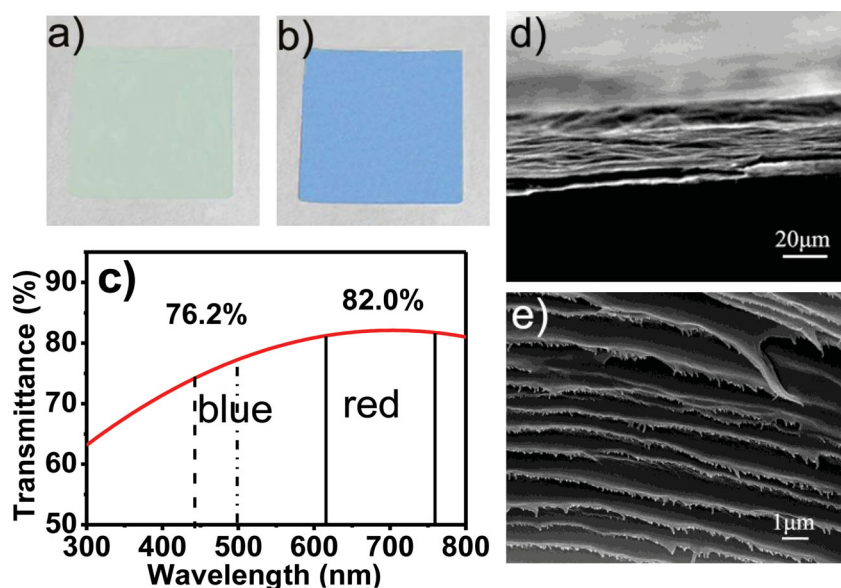


Figure 2. a,b) Photographs of PDA/graphene films before (a) and after (b) 254-nm UV irradiation for 10 s. c) Transmittance of graphene deposited on PET without PDA. d,e) Low- and high-resolution SEM cross-section images of PDA/graphene film after UV irradiation.

Figure 2a and **b** are photographs of the PDA/graphene composite film before and after irradiation with 254-nm UV light. The PDA/graphene film was semitransparent and white before polymerization, and it was transformed to blue after illumination with UV light. This typical color change indicates that PDA is formed upon UV illumination. **Figure 2c** presents the light transmittance in the visible range of our graphene membrane with a thickness of 20 μm , showing an average transmittance of 76.9% in the red-light region and 82% in the blue-light region. Scanning electron microscopy (SEM) images (**Figure 2d,e**) show that the blue-colored film is composed of aligned graphene-sheet lamella. The graphene sheets were assembled into a paper-like membrane under directional flow.

The thickness of the graphene films had a range of $\sim 1\text{--}40$ μm . In a magnified side-view SEM image, the surface of each graphene sheet lamella is clearly coated with a thin layer of soft material. The structure of the PDA/graphene membrane is porous, and there are loose contacts between adjacent laminas (**Figure 2d,e**), which boosts the diffusion of gaseous molecules into the membrane generating more efficient interactions with PDA.

Scanning tunneling microscopy (STM) analysis gives structural details of the PDA/graphene film. Shown in **Figure 3a** and **b** are images before and after polymerization. In **Figure 3a**, a large number of highly aligned idges are observed, each of which consists of parallel stripes, indicating the

formation of an ordered PCDA monomer film on the graphene via a self-assembly procedure. A PCDA molecular chain consists of parallel bright lines separated by two different width intervals, in which the bright and the dark linear areas in the STM images correspond to the π -conjugated backbone and alkyl side chains, respectively. Due to the enhanced electronic charge transfer in the multiple-carbon-bond structures, the diacetylene moiety in the PCDA molecule is brighter than in the alkyl chains. In **Figure 3b**, emergence of regular brighter stripes illustrates the formation of PDA by the UV illumination. In addition to brighter images, the polymers were observed to have a more elevated height profile than that of the monomers due to the lifted-up conformation model.^[31,32] **Figure 3c** and **d** are STM height profiles along the path indicated by the white lines in **Figure 3a** and **b**, respectively. The monomers and polymers in the image are measured to be 0.056 and 0.48 nm tall, respectively.

The investigation of the VOC-induced colorimetric transition of the self-assembled PDA film on graphene is important for the purpose of making portable litmus-type chemosensors. Four typical organic solvents, including tetrahydrofuran (THF), CHCl_3 , CH_3OH , and dimethylformamide (DMF), were chosen for this study. To test the capability of detecting VOCs, our PDA/graphene paper was exposed to

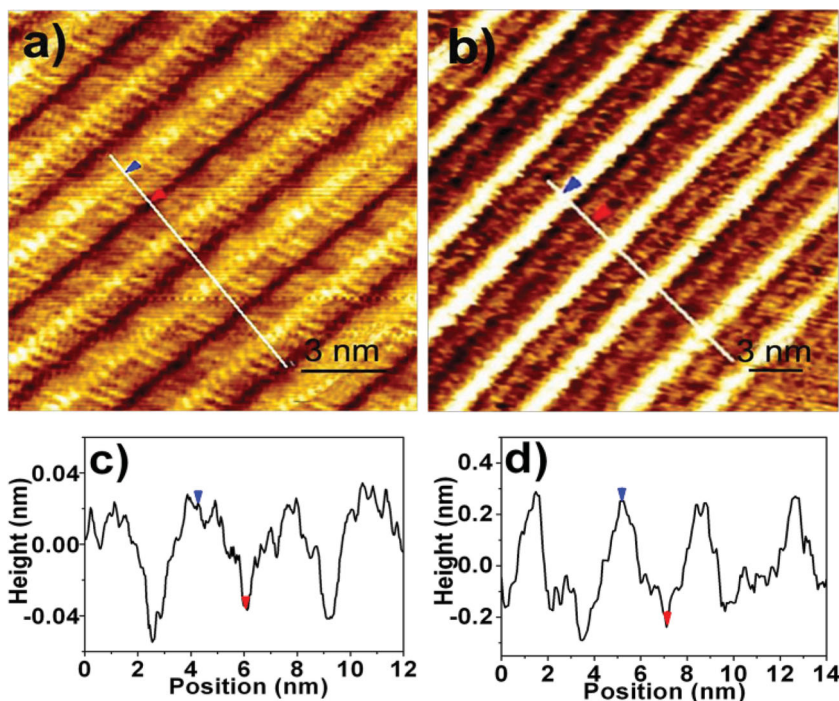


Figure 3. a,b) STM images of PDA/graphene before (a) and after (b) UV irradiation. c,d) Height profiles of the cross-section along the path indicated by the white lines in images a) (c) and b) (d).

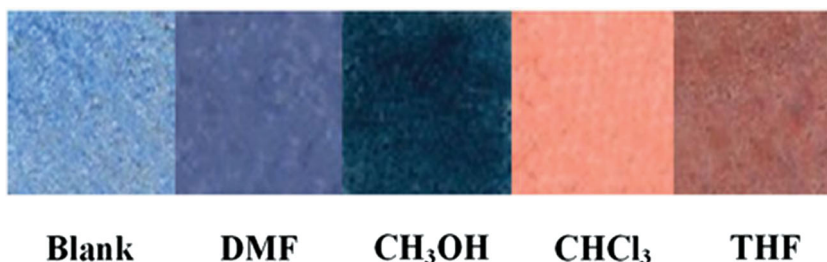


Figure 4. Photographs of the PDA/graphene films after exposure to various organic vapors for 2 min.

organic vapors in a concentration range from 0.01% (percent by volume) to 20% for 2 min. The samples displayed vivid color changes, which are detectable by the naked eye (Figure 4). From visual observations, THF and CHCl_3 are apparently more effective compared to other vapors, in term of disturbing the blue-phase PDA/graphene film. The red-shift from the original blue was observed when the film was exposed to 15% THF (Figure S2, SI) and a complete change to red was observed in 20% THF or 20% CHCl_3 after 2 min of exposure, while no red-phase PDA was observed after exposure to CH_3OH and DMF. Therefore, this self-assembled PDA/graphene stacked paper has a vapor-dependent colorimetric response to organic compounds. The PDA/graphene sensor shows different responses to THF, CHCl_3 , CH_3OH , and DMF, which implies that the sensor has some selectivity, but it cannot separate the contributions if the VOC vapor is a mixture of several chemical gases.

To demonstrate the enhancement of sensing performance by means of the graphene supporter, comparative investigations were carried out on the PDA/graphene composite film and on PDA film on PET substrate using UV-vis spectroscopy (Figure S3 and S4 (SI)). The PDA film on PET was prepared by directly coating diacetylenic precursors onto the substrate, followed by polymerization under UV light. The peak associated with a blue phase appears at ~ 670 nm, while the peaks corresponding to the red phase are at ~ 550 and ~ 500 nm. As shown in the UV-visible spectra (Figure S3 and S4 (SI)), there are concentration changes at the peaks at 670 and ~ 550 nm. The phase change (blue-to-red transition) is quite dramatic with high concentrations (15%, 20%) of THF and CHCl_3 , while very little change was observed in the blue absorption band below a concentration of 1%. This is consistent with previously reported absorption spectra of PDA, in which it interacted with organics or ions in solution at a relatively low concentration range.^[31,32] Based on the UV-vis spectra, the chromatic response (CR) can be quantified, which is defined as the percentage from blue to red. Firstly, the initial (B_0) and final (B_f) blue percent is determined by the formula $(A_{\text{blue}}/[A_{\text{blue}} + A_{\text{red}}]) \times 100\%$, where A is the absorbance values corresponding

to the “blue” or “red” spectra. Then, the chromatic response can be obtained by $\text{CR} = (B_0 - B_f)/B_0 \times 100\%$, and a complete blue-to-red transition has B_f equal to 0 and CR at 100%. In previously reported absorption spectra of PDA, measured after the interaction with organics or ions in solution, the signal peak intensity at ~ 670 nm was gradually weakened accompanied by the emergence of another adsorption peak at 550 nm. The intensity of the 550 nm absorption increases with the concentration of organics or ions.^[33,34] Regardless of

whether PDA is on graphene or PET, when exposed to VOCs (Figure S3 and S4 (SI)), an intensity shift from the blue peak (~ 670 nm) to the red peak (550 nm) is not obvious for relatively low concentrations of VOCs, while the red peak appears clearly in the UV spectrum upon exposure to high concentrations of VOC vapors (e.g., 20% THF). This is possibly due to the fact that the transformation of the conjugate backbone occurs easily in solution, but more difficultly in vapor. The CR data from a wide concentration range can be calculated using a Lorentz Transformation of the UV spectral data. Figure 5 shows the response comparison of PDA/graphene and PDA on PET, in which the x -axis is a logarithmic scale. The concentrations of the four different organic vapors used in this study (THF, CHCl_3 , CH_3OH , and DMF) ranged from 0.01% to 20%. CR values from the sensors of both PDA/graphene film and PDA film on PET increase as they are exposed to increasing concentrations of VOCs. The PDA sensor showed differential response to the four vapors of THF, CHCl_3 , CH_3OH , and DMF; for example, high CR values of 82% and 75.6% were observed

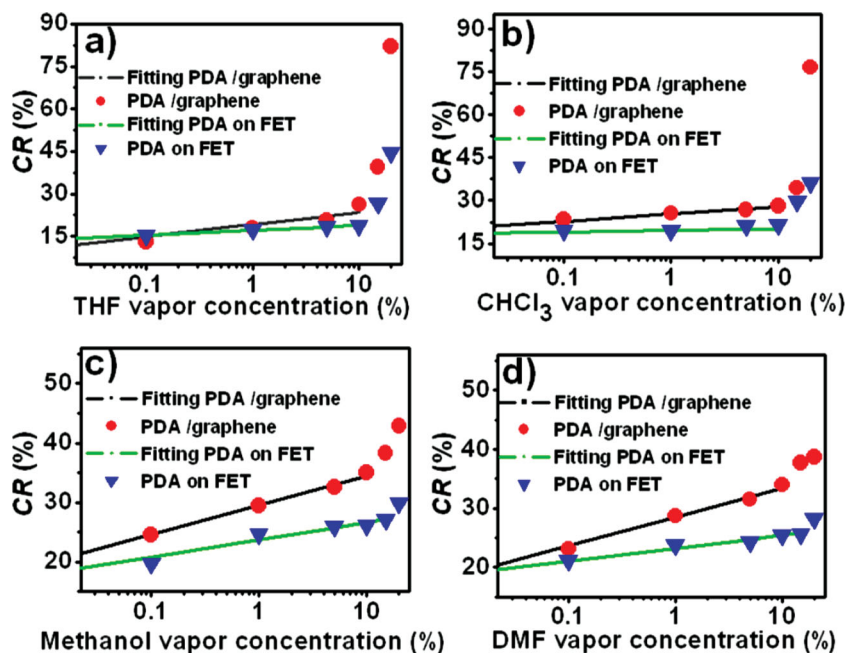


Figure 5. Experimental and fitting curves for chromatic response versus vapor concentration characteristics of PDA/graphene film and PDA film on PET. Red dots and blue triangles are measured data; black or green solid lines are drawn according to Equation 1 in the concentration range of $\sim 0.01\%$ – 10% .

for THF and CHCl_3 , respectively, while the *CR* values were only 42.9% for CH_3OH and 38.7% for DMF. In comparison, the PDA/graphene sensor shows a significant increase in *CR* values compared to the PDA sensor on PET substrate for the four above-mentioned VOCs at the same concentrations. For 20% THF and CHCl_3 , the PDA/graphene film sensor exhibits almost 100% enhancement in *CR* values compared to sensors made of PDA on PET, while the *CR* signals are improved by about 50% for CH_3OH and DMF. At low concentrations, such as 0.1% VOC, the *CR* value improvement is also rather significant as shown in Figure 5. Furthermore, atomic force microscopy (AFM) characterization of PDA on graphene and PET shows that PDA can be assembled into a continuous film on graphene while PDA formed aggregates or discrete flakes on PET (Figure S6 (SI)). The reason why the PDA/graphene on PET is more sensitive than PDA on PET is mainly attributed to the formation of an ordered monolayer of PDA supermolecules on the large surface of the graphene sheet which amplifies the absorbing area for gaseous molecules.

As revealed from Figure 5, we found that the relationship between the *CR* value and the VOC concentration is logarithmic in the VOC concentration range of ~0.01%–10%:

$$CR = B \ln N + C \quad (1)$$

where *B* and *C* are constants, depending on the type of VOCs. This is an important discovery, which makes it possible for PDA sensors to give quantitative values for practical applications. For our graphene/PDA sensor, these constants can be fitted from the measured data in Figure 5 and are given in Table 1 for the four VOCs: THF, CHCl_3 , CH_3OH , and DMF. The corresponding fitting curves are also given as solid lines in Figure 5. With these constants, the concentration can be determined from the formula $N = e^{((CR-C)/B)}$ with the measured value of *CR*. In fact, this formula also can be applied to other types of PDA sensors.

Although research effort has been devoted to determining the reason for the color changes in PDA materials that are caused by VOCs or other stimulating materials, there are still disputes about the mechanism of the blue–red color-change. The popular view is that the color transformation is caused by side-chain fluctuation or conjugate backbone twisting, which was proposed based on the data obtained by indirect methods (theoretical derivation or UV–vis spectroscopy).^[35,36] In this work, we try to reveal the conformation changes of PDA on graphene film upon exposure to VOC vapors by using both STM analysis and UV–vis spectroscopy. Figure 6 shows 3D STM images and molecular models of the arrangement of PDA on graphene after polymerization and exposure to 20% DMF, CH_3OH , CHCl_3 , and THF vapor for 2 min. Figure 6a shows the regular and linear structure of the PDA polymer on the graphene surface without any exposure to VOCs. Figure 6b and c exhibit almost no changes in the backbone structure of the polymer after PDA/graphene is exposed to 20% DMF and 20% CH_3OH , respectively. This indicates that the slight colorimetric change upon exposure to DMF or CH_3OH , are caused by the induced arrangement change of the side-chain groups while maintaining the ordered structure of the polymer backbone (shown in the models of Figure 6b,c). These small movements of side-chain groups can hardly be

Table 1. Constants for Equation 1 obtained by fitting the data of Figure 5 in the concentration range of 0.01–10%.

VOC	PDA/graphene constants		PDA on PET constants	
	B	C	B	C
THF	1.87	19.24	0.73	17.20
CHCl_3	1.13	25.34	0.22	19.56
CH_3OH	2.15	29.56	1.25	23.71
DMF	2.14	28.54	0.95	23.23

distinguished by STM observation, but they can be easily detected by UV–vis spectroscopy (Figure S3b,c of the SI and in Figure 4). Figure 6d shows a STM image after exposure to 20% CHCl_3 , where one can see that the polymer backbones along white lines are partially twisted. The polymer backbones shown in this image are wider than those of PDA without exposure to VOCs (Figure 6a), which is due to the twisting of side-chains that largely shorten the distance between two adjacent polymer backbones (shown in the model of Figure 6d). A 3D STM image of the PDA/graphene structure after exposure to 20% THF is given in Figure 6e, which shows that the regular structure is completely replaced by distorted and overlapped areas. Both conjugated backbones and side-chains are distorted after exposure to THF. These huge changes in the polymer backbone and the side-chains, which are revealed by STM, are the molecular origin of the apparent blue–red color change; it can also be detected by the UV–vis spectroscopy (Figure S3a,b (SI)) and even by the naked eye (Figure 4). In other words, the blue and red color variety of PDA originates from side-chain fluctuation upon exposure to DMF and CH_3OH , while both the conjugate backbone twisting and side-chain fluctuations contribute to the color change in PDA when it is exposed to CHCl_3 and THF. Our STM study gives, for the first time, direct evidence for the mechanism of the colorimetric change in PDA molecules.

3. Conclusion

In summary, a portable and sensitive colorimetric sensor has been developed using PDA/graphene paper. Graphene in the paper acts as an efficient supporter of a self-assembled PDA film owing to its large surface-to-volume ratio and good transparent properties, which enhances the sensitivity of the PDA sensor. The vapor of four different VOCs—THF, CHCl_3 , CH_3OH , and DMF—were used as testing samples. The PDA/graphene-based sensor shows a concentration-dependent response to these four VOCs. The minimum concentration that can be detected is as low as 0.01%. At a relatively high concentration, the colorimetric response could even be perceived by the naked eye. In the concentration range of ~0.01%–10%, an analytic formula has been obtained for the four VOCs by fitting the experimental data, which makes it possible for our PDA/graphene sensors to give quantitative indication of the VOC concentration. The structural changes of the PDA molecules caused by its interaction with VOCs were directly observed using 3D STM, which provides solid evidence for the mechanism of chromatic changes in PDA upon exposure to VOC vapors.

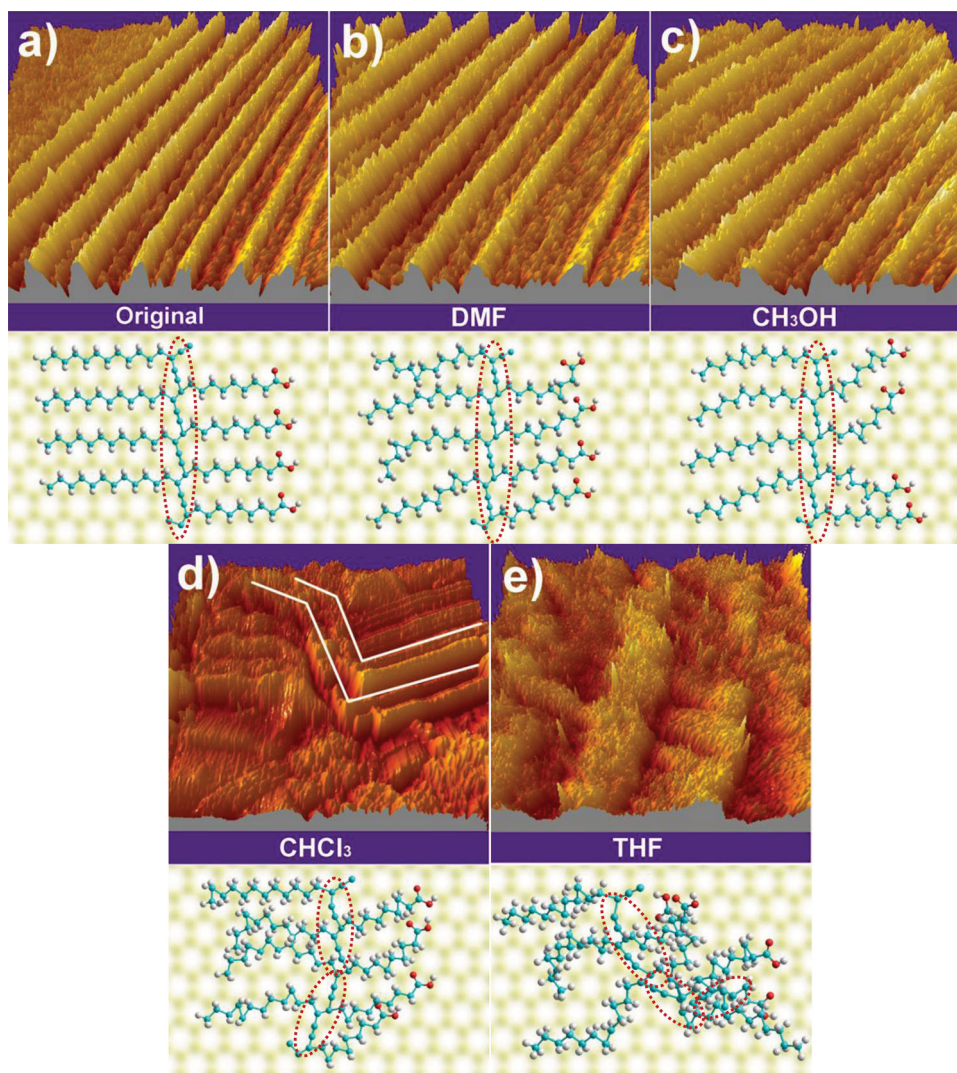


Figure 6. 3D STM images (top) and corresponding molecular arrangement model (bottom) of PDA/graphene film a) before exposure to VOCs and b–e) after exposure to 20% DMF (b), CH₃OH (c), CHCl₃ (d), and THF (e) vapors for 2 min. The conjugate backbone is highlighted by the red dotted line. Imaging conditions: a) Sample bias voltage $V_s = 1.0$ V, tunneling current $I_t = 0.015$ nA, scanning area $S = 38$ nm \times 38 nm; b) $V_s = 0.5$ V, $I_t = 0.6$ nA, $S = 28$ nm \times 28 nm; c) $V_s = 1.2$ V, $I_t = 0.6$ nA, $S = 28$ nm \times 28 nm; d) $V_s = 1.0$ V, $I_t = 0.025$ nA, $S = 45$ nm \times 45 nm; e) $V_s = -1.0$ V, $I_t = 0.07$ nA, $S = 100$ nm \times 100 nm.

4. Experimental Section

Materials: PCDA was purchased from GFS Chemical, and natural flake graphite and other reagents were purchased from Sigma-Aldrich. Analytical grade solvents such as THF, CHCl₃, CH₃OH, and DMF were used without further purification. SEM was carried out using a Hitachi S-4200 with an accelerating voltage of 10 kV. STM images were performed using a Digital Instruments NanoScope STM system. All images were recorded under ambient conditions using Pt-Ir tips in the constant-current mode. AFM images were acquired using the tapping mode with a commercial multimode Nanoscope IIIa (Veeco Co. Ltd). Raman spectra were collected with a LabRAM XploRA laser Raman spectrometer (HORIBA Jobin Yvon CO. Ltd) using a 532 nm laser with an incident power of 0.15 mW. The optical photographs were obtained using a Canon EOL 60D SLR camera. The absorption spectra were measured using a Hitachi U-4100 spectrophotometer.

Preparation of Graphene: Natural flake graphite was loaded into a fused silica tube and heated to 1000 °C under H₂:Ar at 50:450 sccm (standard-state cubic centimeter per minute) for 2 min. Then, the calcined graphite was dispersed in the DMF solvent (0.1 mg mL⁻¹) by sonicating for 60 min. The mixture was then centrifuged at 1000 rpm for 90 min to obtain a stable dispersion of graphene nanosheets. After centrifugation, the low-density material that was suspended in the top layer of the dispersion was collected. The dispersion of graphene sheets were deposited onto PET substrates by a “drop and dry” process.

Preparation of PDA/Graphene Film: PDA monomers, 10,12-pentacosadiynoic acid (PCDA) (10 mg), was dissolved in chloroform (1 mL) and filtered to remove any pre-polymerized material. The colorless solution was dropped onto graphene film and exposed to open air for 24 h in the dark in order to evaporate the solvent. Diacetylenic moieties were polymerized at room temperature under UV light with a wavelength of 254 nm for 10 s to 5 min. The film was white

before polymerization as a result of the PDA monomers and it became blue after polymerization.

Supporting Information

Supporting Information is available from the Wiley Online Library or from the author.

Acknowledgements

This work is supported by the National Key Basic Research Program of China (973 Program) under Grant No. 2013CB632900, the National Natural Science Foundation of China (NSFC, No. 61172001), and the Chinese Program for New Century Excellent Talents in University.

Received: March 26, 2013

Revised: May 9, 2013

Published online: July 26, 2013

- [1] A. Sun, J. W. Lauher, N. S. Goroff, *Science* **2006**, *312*, 1030–1034.
- [2] Y. Lu, Y. Yang, A. Sellinger, M. Lu, J. Huang, H. Fan, R. Haddad, G. Lopez, A. R. Burns, D. Y. Sasaki, *Nature* **2001**, *410*, 913–917.
- [3] Y. Okawa, M. Aono, *Nature* **2001**, *409*, 683–684.
- [4] B. Yoon, S. Lee, J. M. Kim, *Chem. Soc. Rev.* **2009**, *38*, 1958–1968.
- [5] L. Motiei, M. Lahav, D. Freeman, M. E. Boom, *J. Am. Chem. Soc.* **2009**, *131*, 3468–3469.
- [6] H. S. Peng, J. Tang, L. Yang, J. Pang, H. S. Ashbaugh, C. J. Brinker, Z. Z. Yang, Y. F. Lu, *J. Am. Chem. Soc.* **2006**, *128*, 5304–5305.
- [7] D. J. Ahn, J. M. Kim, *Acc. Chem. Res.* **2008**, *41*, 805–816.
- [8] T. Kida, M. H. Seo, S. Kishi, Y. Kanmura, N. Yamazoe, K. Shimanoe, *Anal. Chem.* **2010**, *82*, 3315–3319.
- [9] J. Yoon, S. K. Chae, J. M. Kim, *J. Am. Chem. Soc.* **2007**, *129*, 3038–3039.
- [10] D. J. Ahn, J. M. Kim, *Acc. Chem. Res.* **2008**, *41*, 805–816.
- [11] C. Elosua, I. R. Matias, C. Barriain, F. J. Arregui, *Sensors* **2006**, *6*, 1440–1465.
- [12] T. Kida, H. Harano, T. Minami, S. Kishi, N. Morinaga, N. Yamazoe, K. Shimanoe, *J. Phys. Chem. C* **2010**, *114*, 15141–15148.
- [13] K. Tian, D. Hu, R. Hu, S. Wang, S. Li, Y. Li, G. Yang, *Chem. Commun.* **2011**, *47*, 10052–10054.
- [14] L. Silbert, I. B. Shlush, E. Israel, A. Porgador, S. Kolusheva, R. Jelinek, *Appl. Environ. Microbiol.* **2006**, *72*, 7339–7344.
- [15] Y. Gu, W. Cao, L. Zhu, D. Chen, M. Jiang, *Macromolecules* **2008**, *41*, 2299–2303.
- [16] J. M. Kim, Y. B. Lee, S. K. Chae, D. J. Ahn, *Adv. Funct. Mater.* **2006**, *16*, 2103–2109.
- [17] H. Jiang, Y. L. Wang, Q. Ye, G. Zou, W. Su, Q. J. Zhang, *Sens. Actuators, B* **2010**, *143*, 789–794.
- [18] A. D. Nava, M. Thakur, A. E. Tonelli, *Macromolecules* **1990**, *23*, 3055–3063.
- [19] J. M. Kim, J. S. Lee, H. Choi, D. Sohn, D. J. Ahn, *Macromolecules* **2005**, *38*, 9366–9376.
- [20] D. J. Ahn, E. H. Chae, G. S. Lee, H. Y. Shim, T. E. Chang, K. D. Ahn, J. M. Kim, *J. Am. Chem. Soc.* **2003**, *125*, 8976–8977.
- [21] Q. Nie, Y. Zhang, J. Zhang, M. Zhang, *J. Mater. Chem.* **2006**, *16*, 546–549.
- [22] B. A. Pindzola, A. T. Nguyen, M. A. Reppy, *Chem. Commun.* **2006**, 906–908.
- [23] M. A. Reppy, B. A. Pindzola, *Mater. Res. Soc. Symp. Proc.* **2006**, *942*, W13–10.
- [24] T. Eaidkong, R. Mungkarndee, C. Phollookin, G. Tumcharern, M. Sukwattanasinitt, S. Wacharasindhu, *J. Mater. Chem.* **2012**, *22*, 5970–5977.
- [25] X. L. Li, H. L. Wang, J. T. Robinson, H. Sanchez, G. Diankov, H. J. Dai, *J. Am. Chem. Soc.* **2009**, *131*, 15939–15944.
- [26] R. Giridharagopal, K. F. Kelly, *ACS Nano*. **2008**, *2*, 1571–1580.
- [27] R. Giridharagopal, K. F. Kelly, *J. Phys. Chem. C* **2007**, *111*, 6161–6166.
- [28] W. X. Xue, D. Q. Zhang, G. X. Zhang, D. B. Zhu, *Chin. Sci. Bull.* **2011**, *56*, 1877–1883.
- [29] J. S. Yun, K. S. Yang, D. H. Kim, *J. Nanosci. Nanotechnol.* **2011**, *11*, 5663–5669.
- [30] U. Khan, H. Porwal, A. O'Neill, K. Nawaz, P. May, J. N. Coleman, *Langmuir* **2011**, *27*, 9077.
- [31] T. Champai boon, G. Tumcharern, A. Potisatityuengyong, S. Wacharasindhu, M. Sukwattanasinitt, *Sens. Actuators, B* **2009**, *139*, 532–537.
- [32] D. A. Jose, S. Stadlbauer, B. Konig, *Chem. Eur. J.* **2009**, *15*, 7404–7412.
- [33] Y. J. Okawa, D. Takajo, S. Tsukamoto, T. Hasegawaabc, M. Aonob, *Soft Matter* **2008**, *4*, 1041–1047.
- [34] Y. Okawa, M. Aono, *J. Chem. Phys.* **2001**, *115*, 2317–2323.
- [35] D. J. Ahn, E. H. Chae, G. S. Lee, H. Y. Shim, T. E. Chang, K. D. Ahn, *J. Am. Chem. Soc.* **2003**, *125*, 897.
- [36] Z. Yuan, C. W. Lee, S. H. Lee, *Angew. Chem. Int. Ed.* **2004**, *43*, 4197–4200.